ABSTRACT

Title of Thesis: IMPACT OF SALINITY ON MORPHOLOGY, GROWTH, AND PIGMENT PROFILES OF SCENEDESMUS OBLIQUUS HTB1 UNDER AMBIENT AIR AND ELEVEATED CO2 (10%) CONDITIONS

Fanglue Jiao, Master of Science, 2025

Thesis Directed By: Professor, Feng Chen, IMET, UMCES

Certain microalgal species tolerate high CO_2 concentrations and proliferate faster with elevated CO_2 than with ambient air. This feature makes them attractive for carbon sequestration, a tool for mitigating climate change due to increasing atmospheric CO_2. *Scenedesmus* species are among these microalgae. *Scenedesmus obliquus* strain HTB1 is a microalgal strain isolated from the Baltimore Inner Harbor (brackish water) and has shown a faster growth with 10% CO_2 compared to air. However, how HTB1 grows under different salinity and if the salt response is affected by elevated CO_2 remains elusive. Two experiments were set up to address these questions. The first experiment tested the impact of salinity gradient (0, 17.5, 20, 22.5, 25, 27.5, and 30 ppt) on HTB1 under ambient air. With increasing salinity, HTB1 cells became smaller, and the cultures changed color from green to brown, yellowish brown, and then to pale white. The pigment analysis showed that HTB1 reduced several pigments (i.e. zeaxanthin, lutein, chlorophyll *b*) in response to salt stress. However, HTB1 produced higher concentrations of canthaxanthin under

the salt stress. The growth of HTB1 decreased with increasing salinity and was inhibited when the salinity was greater than 22.5 ppt. In the second experiment, we compared the impact of salinity (0, 10, and 20 ppt) on HTB1 under air and 10% CO_2, respectively. HTB1 cultures showed little color change with increasing salinity under 10% CO_2. In contrast, the change of culture color from dark green to brown was observed with increasing salinity when HTB1 was grown with air. Interestingly, the growth of HTB1 was less inhibited with salt under 10% CO_2 than with air, suggesting that elevated CO_2 mitigates the salt stress of HTB1. Lutein and canthaxanthin increased with increasing salinity when HTB1 was grown with 10% CO_2. Our results indicate that increased salinity has more of a negative effect on the growth of *Scenedesmus obliquus* HTB1 when grown with air than with 10% CO_2. This study provides insight into the impact of salt stress on algal morphology, growth, and pigment composition.

IMPACT OF SALINITY ON MORPHOLOGY, GROWTH, AND PIGMENT PROFILES OF SCENEDESMUS OBLIQUUS HTB1 UNDER AMBIENT AIR AND ELEVEATED CO2 (10%) CONDITIONS

by

Fanglue Jiao

Thesis submitted to the Faculty of the Graduate School of the
University of Maryland, College Park, in partial fulfillment
of the requirements for the degree of
Master of Science
2025

Advisory Committee:
Professor Feng Chen, Chair
Yantao Li
Elizabeth North

Acknowledgments

We acknowledge the funding support from the U.S. Department of Energy Office of Fossil Energy and Carbon Management (FE-0031914, FE-0032188). This work was also supported by the funding from National Science Foundation Convergence Accelerator (ITE-2344228), the Maryland Industrial Partnership Program, the Maryland Department of Natural Resource, HY-TEK Bio, LLC, and BetterFedFoods, LLC. (NoA#4701, #5214, #5417, #5903, #6511, #6801, and #7042).

Table of Contents

List of Figures

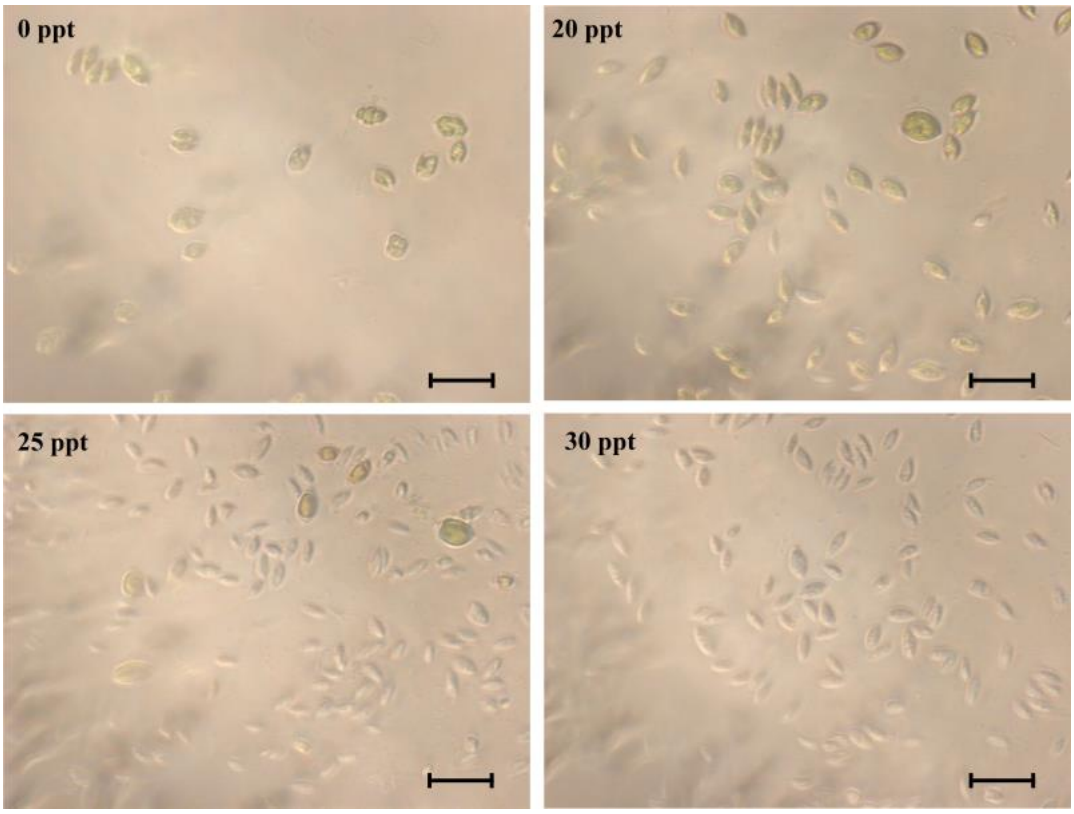

Figure 1. Effect of salinity on the morphology, cell size, and growth of *S. obliquus* HTB1. Brightfield microscopy images showing HTB1 cells grown under four different salt concentrations (0, 20, 25, and 30 ppt) on day 10.

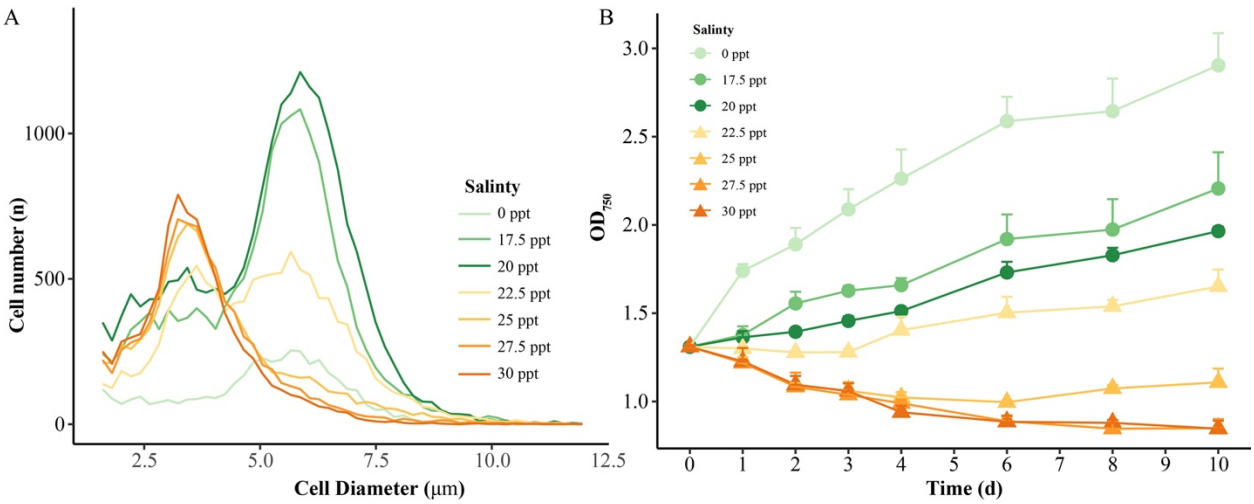

Figure 2. Effect of salinity on the morphology, cell size, and growth of *S. obliquus* HTB1. Panel A presents Coulter counter data, showing the variations of HTB1 cell size under 7 different salinities on the same day. Panel B shows the growth of HTB1 (measured by OD_{750}, mean +/- 1 std, n=3) at 7 different salinities over 10 days.

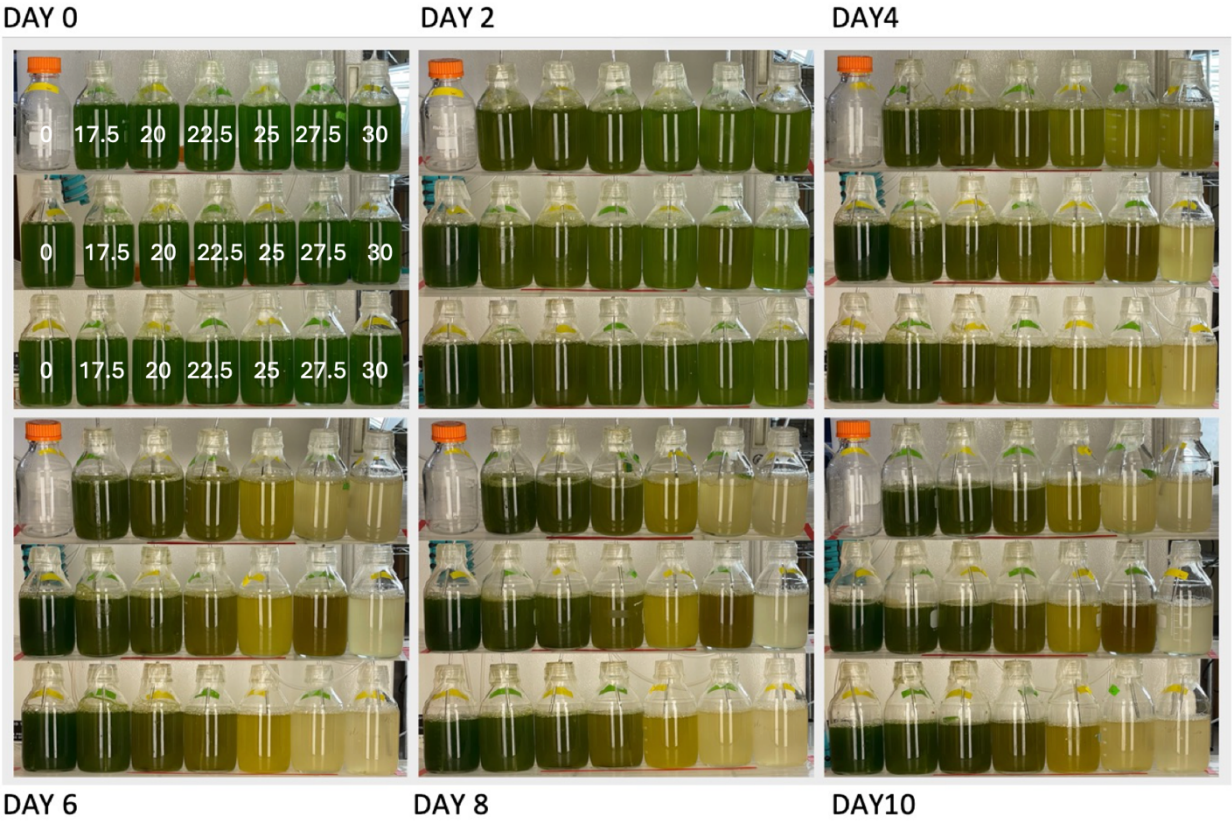

Figure 3. Photographs showing the color of HTB1 grown in different salinities (0, 17.5, 20, 22.5, 25, 27.5, 30 ppt) over 10 days. n=3 (The first bottle was empty due to insufficient algal biomass).

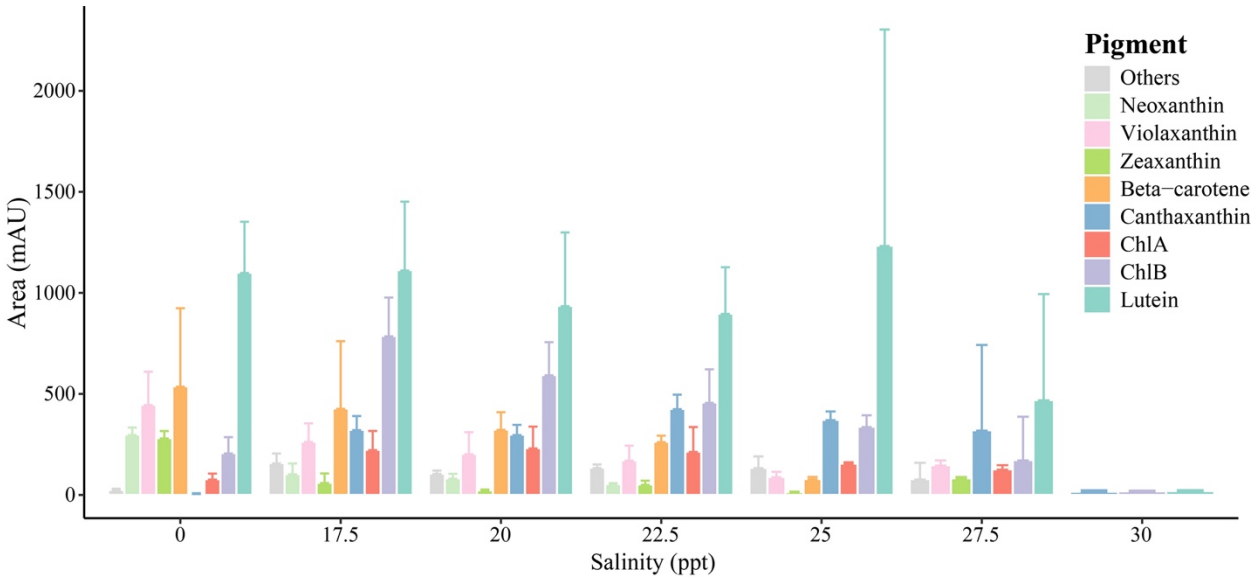

Figure 4. Effects of salinity gradient on pigment abundance (mean area +/- 1 std, n=3) in *Scenedesmus obliquus* HTB1 cultures. The abundance of dominant pigments under different salinity levels after 10 days is shown.

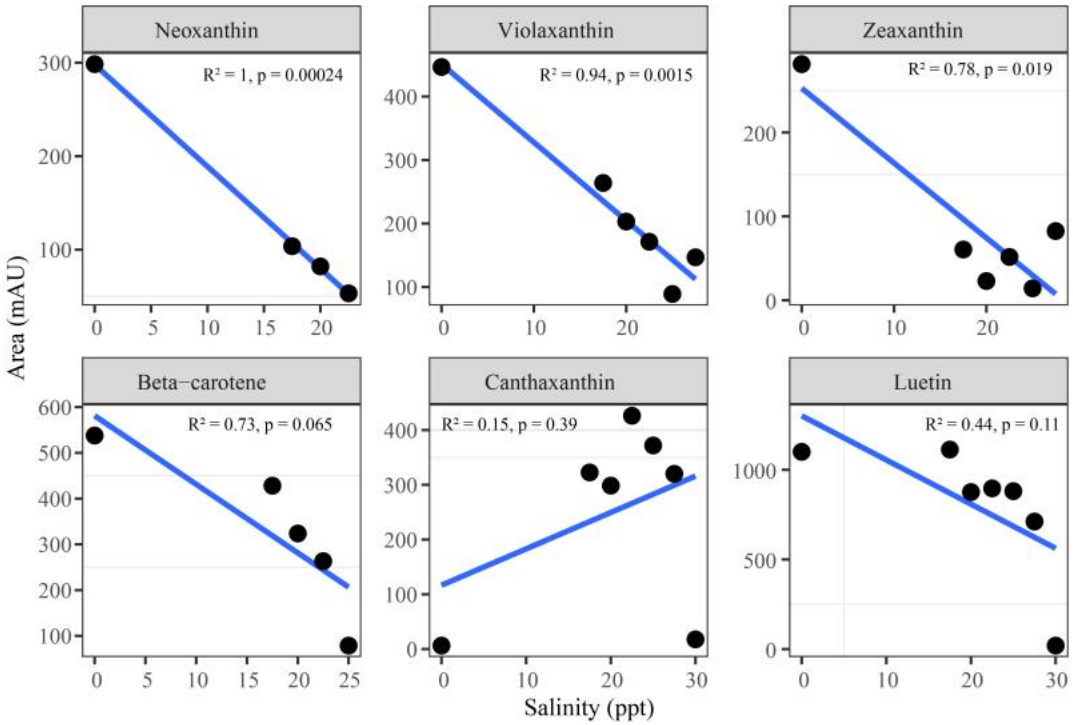

Figure 5. Effects of salinity gradient on pigment abundance in *Scenedesmus obliquus* HTB1 cultures after 10 days. The correlations between each pigment and salinity are shown here. Each data point is the mean of three replicates.

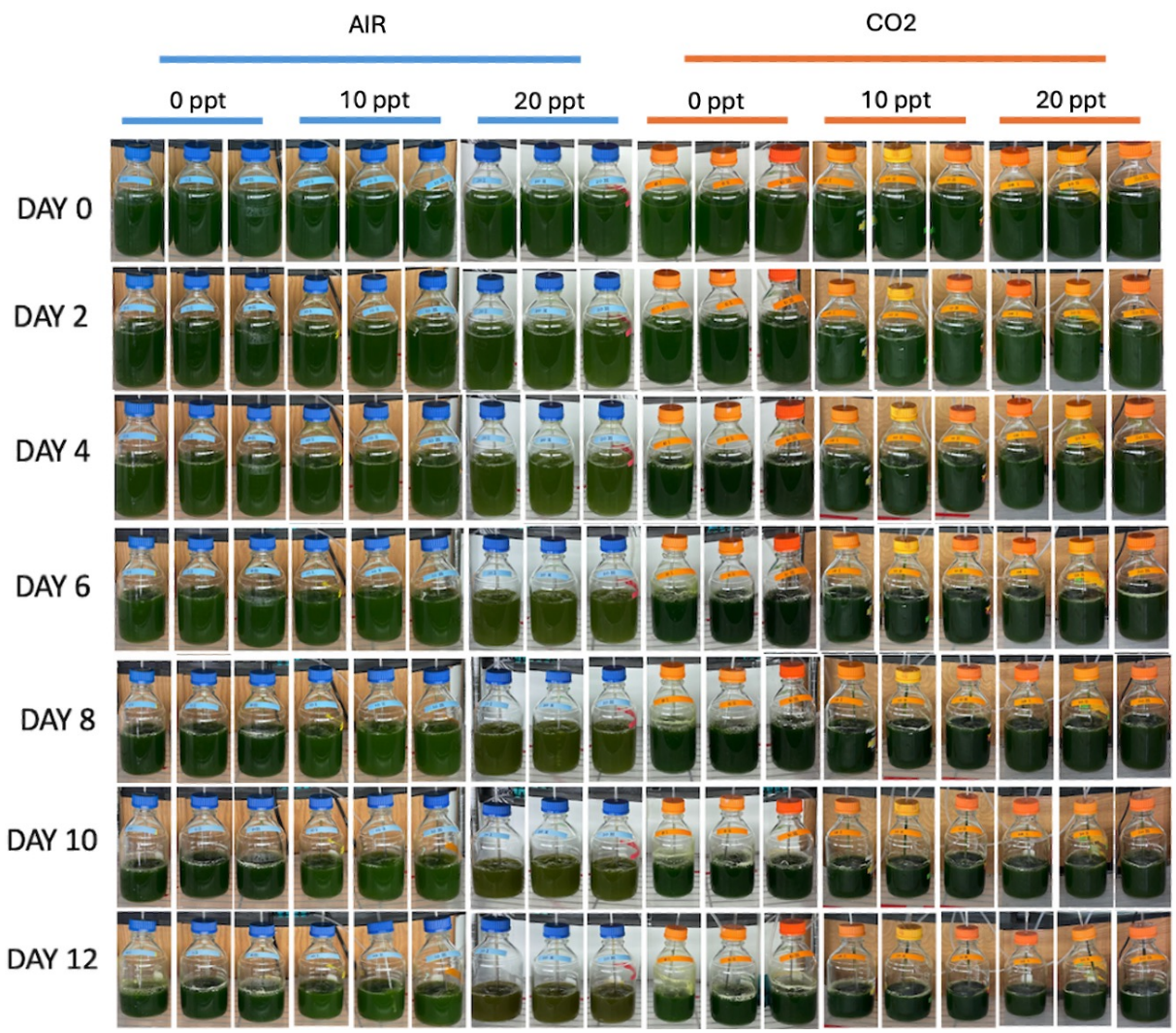

Figure 6. Photographs showing the results of the subsequent *S. obliquus* HTB1 salinity experiment conducted under two conditions: 10% CO_2 and ambient air. The bottles with blue are for the "AIR" group, and the orange caps are for the "CO_2" group. Three salinity levels 0, 10, and 20 ppt were tested. Based on prior experimental results, 20 ppt was considered the high end of salinity level. Each treatment has triplicates. The volume lost is due to daily subsampling.

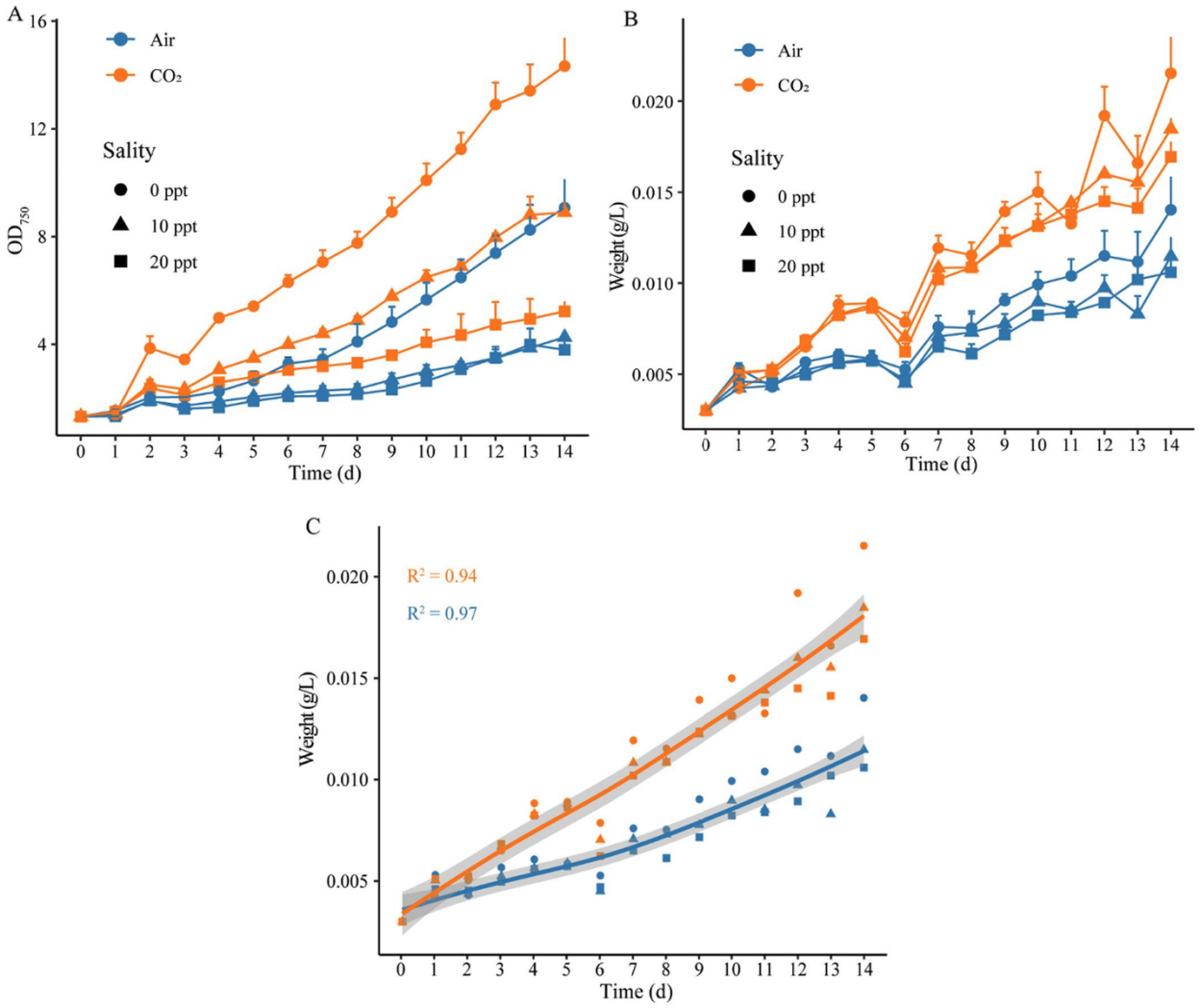

Figure 7. The growth of *S. obliquus* HBT1 under 3 different salinities (0, 10 and 20 ppt) with air and 10% CO_2, respectively, measured by OD_{750} (A) and ash-free dry weight (B) over 14 days (mean +/- 1 std, n=3). Panel C compares the growth of HTB1 under air and 10% CO_2 with all salinity data. Lines are smoothed fits to the data with 95% confidence intervals (gray shaded areas).

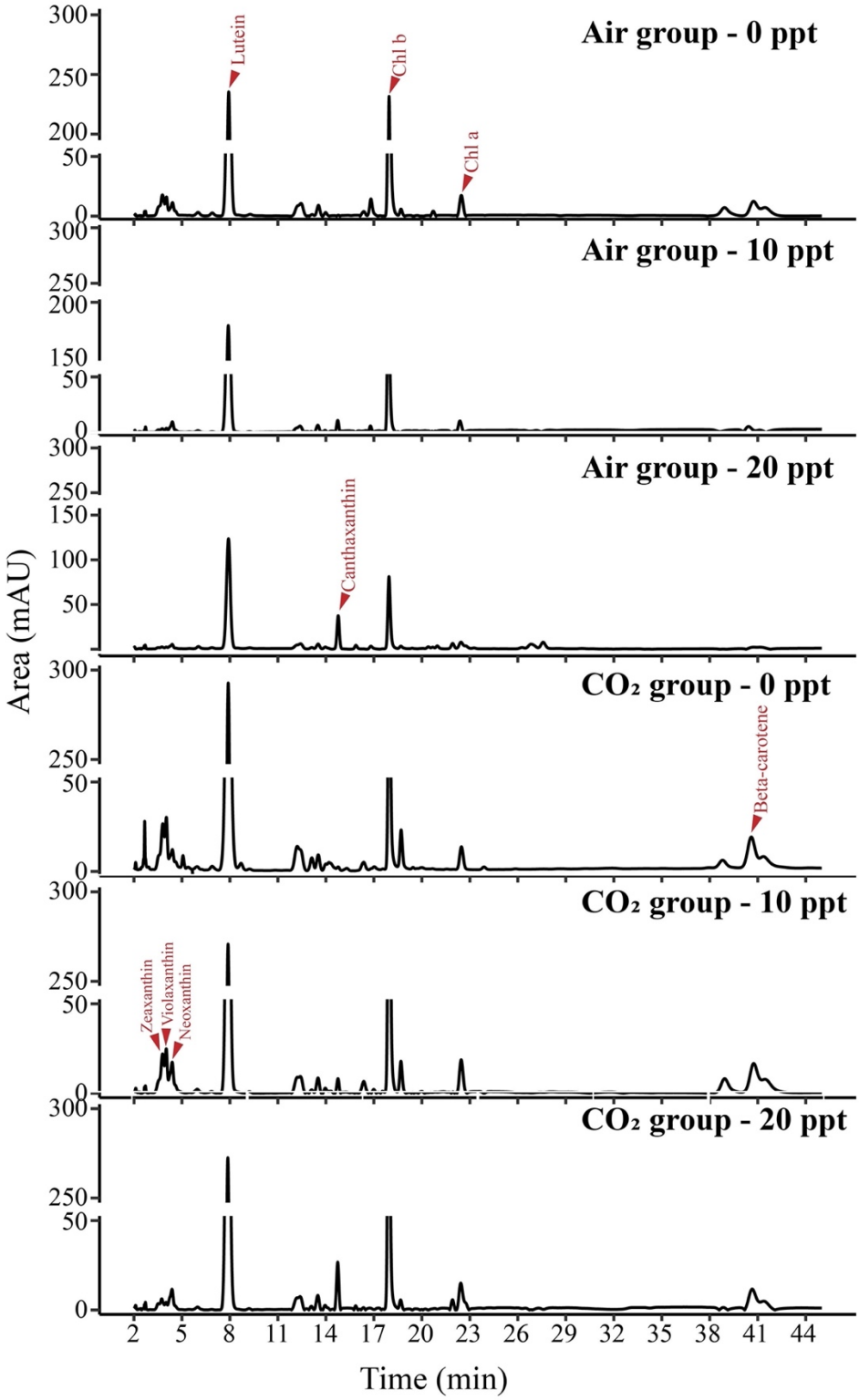

Figure 8. HPLC chromatograms and pigment profiles of *S. obliquus* HTB1 under ambient air and elevated 10% CO_2.after 14 days.

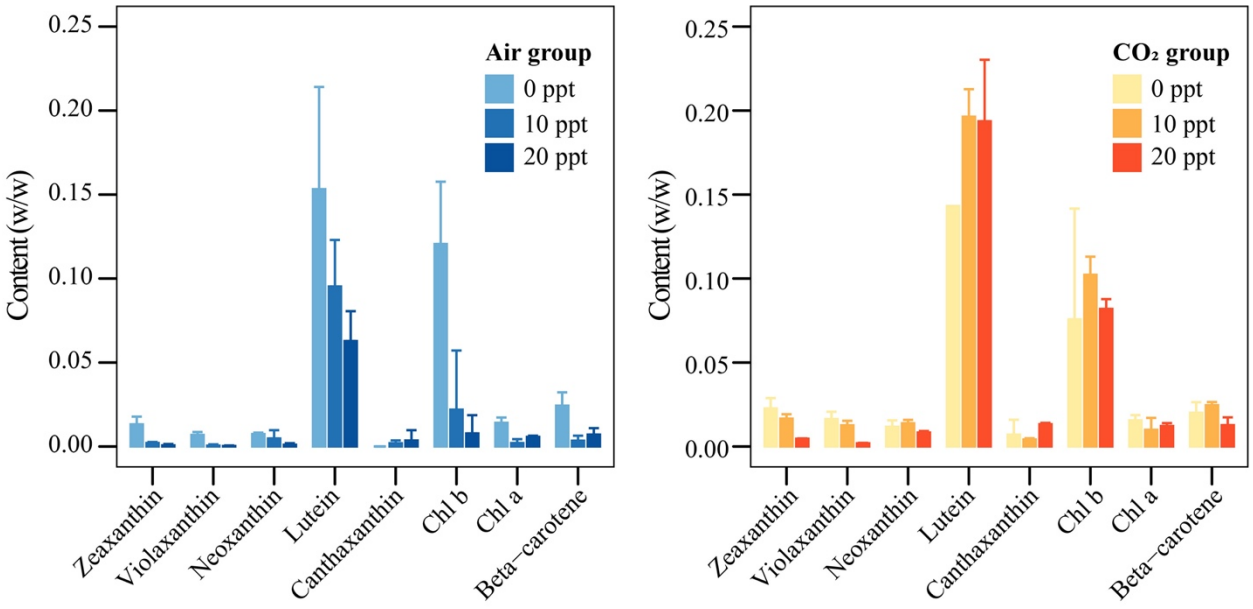

Figure 9. Pigment content (w/w, mean +/- 1 std, n = 3) of major pigments across salinity levels in air (A) and 10% CO_2 (B) treatments after 14 days.

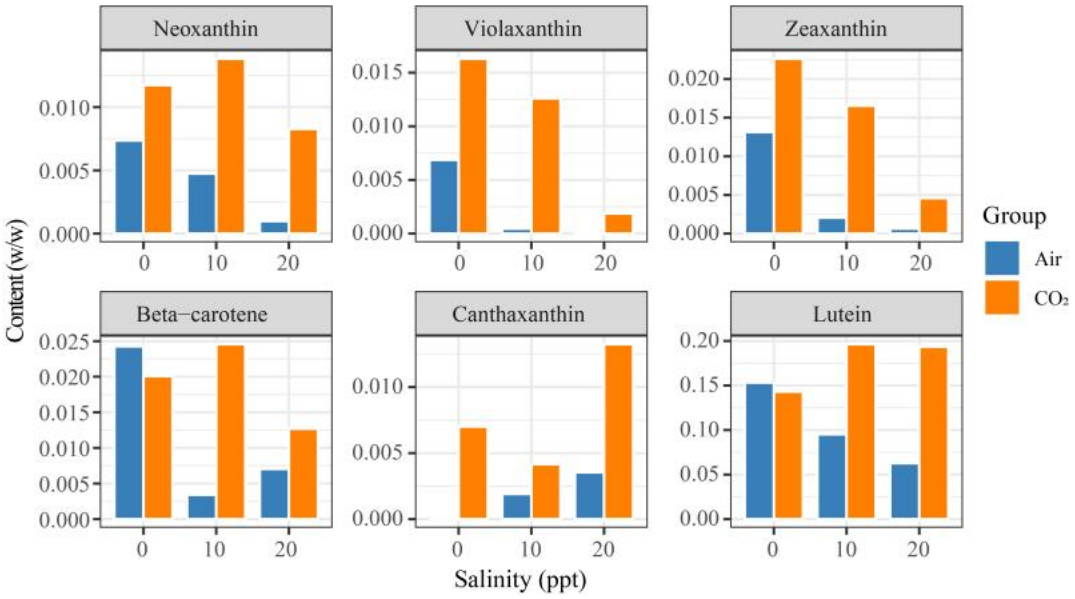

Figure 10. Effect of salinity on pigment yields in *Scenedesmus obliquus* HTB1: Comparative analysis of major pigments under air and 10% CO_2 conditions after 14 days. Note the differences in Y-axis scales between panels.

1. Introduction

Microalgae are the key carbon fixers in nature and important food sources in the food chain. Certain algal species inherit specific characteristics, making them valuable for health product development, carbon sequestration, and wastewater remediation [1]. For instance, microalgae like *Scenedesmus obliquus* are known for their rapid growth and high photosynthetic efficiency, making them promising candidates for various applications, including pigment and biofuel production [2,3]. Certain microalgae are rich sources of pigments and compounds with significant potential in developing health-oriented natural products [4,5]. Culture conditions are often manipulated to enhance the yield of these valuable products [6,7], with common factors influencing algal growth including light, nutrient availability, temperature, pH, CO_2 concentration, and salinity [6]. Salinity stress, CO_2 and nutrient scarcity are frequently applied to boost lipid accumulation [8,9]. Notably, green microalgae species like *S. obliquus*, *Acutodesmus dimorphus*, and *Chlorella vulgaris* show elevated lipid production under increased salinity conditions [10–13]. On the other hand, high salinity can damage the integrity of microalgal cell membranes [14]. In general, the effects of both salinity and CO_2 on the pigment composition of microalgae remain less studied.

Many green microalgae can tolerate high concentrations of CO_2 making them ideal candidates for removing CO_2 in power plant flue gas. There is growing interest in understanding how photosynthetic organisms such as plants and microalgae adapt to elevated CO_2, with studies highlighting changes in carbon fixation, morphology, and metabolic properties [15–17]. While these mechanisms are common across species, *S. obliquus* shows robust growth and metabolic flexibility under elevated CO_2, making it an ideal species for exploring their carbon capture applications. Industrial processes, particularly power and cement production, contribute

substantially to atmospheric CO_2 [18]. Microalgae present a promising solution for mitigating CO_2 emissions in flue gas [18–20]. In addition to their carbon capture benefits, algal biomass can yield economically valuable bioproducts such as biofuels and biochemicals, which can offset carbon mitigation costs [18,20].

Species within the genus *Scenedesmus,* belong to the class Chlorophyceae within the green algae phylum [21]. They are renowned for their ability to thrive in diverse environmental conditions, making them robust and adaptable microalgae [22,23]. These species are characterized by rapid growth and high photosynthetic efficiency, positioning them as prime candidates for applications in pigment and biofuel production [2,3]. *S. obliquus*, in particular, demonstrates exceptional growth under elevated CO_2, reaching a specific growth rate of 1.28 d^{-1}, productivity of 0.28 g L^{-1} d^{-1}, and a theoretical CO_2 fixation rate of 0.56 g L^{-1} d^{-1} at 10% CO_2 [14]. Under salinity stress conditions, *S. obliquus* displays enhanced growth and lipid accumulation when supplemented with CO_2, indicating that CO_2 enrichment may alleviate salinity-induced stress and promote biomass production [24]. A previous study notably reported that increased salinity, combined with CO_2 supplementation, promoted the growth of *Scenedesmus obliquus* [14].

S. obliquus strain HTB1 was isolated from the Baltimore Inner Harbor where salinity varies from 0-20 ppt. Previous studies found that HTB1 can grow in a wide range of CO_2 concentrations and grow faster with 10% CO_2 than air [17,25]. Another study demonstrated that HTB1 also proliferates with nutrients extracted from chicken manure [26]. In addition, HTB1 grows well in large bioreactors charged with power plant flue gas (data not shown). HTB1 has been used to explore its industrial potential for CO_2 mitigation. In this study, we investigated how *S. obliquus* HTB1 responds to the salinity change and the impact of salt stress on HTB1 under both air and

10% CO_2 conditions. The overall goal is to understand how the change in salinity affects the morphology, growth, and pigment composition of *S. obliquus* HTB1.

2. Materials and Methods

2.1 Culture preparation and growth monitoring

S. obliquus strain HTB1 was cultivated and maintained in our laboratory using BG11 medium [25]. For the first experiment, a 12 L culture of HTB1 was scaled up in BG11 medium. For the salinity test, BG11 media with different salinity levels (0, 17.5, 20, 22.5, 25, 27.5, and 30 ppt) were prepared. Each salinity condition was tested in triplicate. A total of 21 culture bottles were set up each containing 500 mL HTB1 culture (Fig. 3). The 0 ppt condition served as the control. The starting optical density (OD_{750}) of HTB1 culture was 1.3. For the second experiment, salinity gradients of 0, 10, and 20 ppt were tested. The seed culture was prepared following the procedure described for the first experiment. Eighteen bottles (1L) were divided into two treatments (n=3), with air or 10% CO_2. Nine bottles were supplied with 10% CO_2, while the other nine were aerated with filtered ambient air. The CO_2 level was monitored and regulated by a CO_2 sensor (GasLab model CM-0121). Ambient air and CO_2 were mixed through a Brooks Instrument Flow Controller to achieve 10% CO_2. The CO_2 concentration was measured constantly with GasLab v2.3.1.4 port COM4.

HTB1 was grown at room temperature (25 °C) with a light intensity of 100 μmol photons m^{-2} s^{-1}. A subsample (15 ml) was taken for growth measurement. Both ash-free dry weight (AFDW) and OD_{750} were measured.

2.2 Growth and cell size measurement

Morphological observations of HTB1 were performed using a Zeiss light microscope (Axioplan, 2012 model, West Germany) to evaluate cell shape and size across different salinity treatments. For cell counting and size distribution, 0.2 μL of culture was mixed with 10 mL of filtered IsoFlow

Sheath Fluid in a Coulter counter cuvette and analyzed using a Beckman Coulter Counter (Multisizer 4e, Coulter counter) under default settings.

The growth rate of HTB1 was monitored daily over 10 days using a spectrophotometer (Superkent Instrument model S-1000) by measuring OD_{750}.

To determine ash-free dry weight (AFDW), 5 mL of culture was filtered through 0.47 μm filters. The filters were dried overnight in an oven (Model 10 lab oven, Quincy Lab, Inc), and measured using an analytical scale (Mettler Toledo AT201). Subsequently, the filters were incinerated in a muffle furnace (Thermolyne, Thermo Scientific) at a high temperature (490 °C) for 30 minutes to remove organic matter. After cooling, the remaining ash-free dry weight was measured using the same analytical scale.

2.3 Pigment analysis using HPLC

Freeze-dried biomass (0.012 mg) was collected for each treatment and placed in a mortar with approximately 1 mL of extraction solvent (dichloromethane, 25:75 v/v). The cells were ground at least three times using liquid nitrogen. The mortar and pestle were rinsed with additional extraction solvent, and all liquids were transferred to a 12 mL glass vial. The samples were centrifuged at 2,000 g for 10 minutes to pellet the cell debris, and the supernatant was transferred to a fresh 12 mL glass tube, and then dried under a nitrogen stream. Once fully dried, 1 mL of extraction solvent was added to re-dissolve the pigments. The solution was filtered through a 0.20 μm Hydrophobic Fluoropore membrane (Merck KGaA, Darmstadt, Germany) into a measurement vial. For HPLC analysis, the mobile phase consisted of two solvents: solvent A (dichloromethane:methanol:acetonitrile, 5:85:5.5:4.5 v/v) and solvent B (dichloromethane:methanol:acetonitrile, 25:28:42.5:4.5 v/v). The mobile phase was set to 100% solvent A from 0 to 8 minutes. From 8 to 14 minutes, solvent A decreased from 100% to 0%, while

solvent B increased from 0% to 100%. Solvent B remained at 100% from 14 to 60 minutes. Samples were run through a HiChrom Ultrasphere 5 μ ODS column (4.6 x 250 mm) (HiChrom Limited, Berkshire, UK) and detected at 480 nm. Astaxanthin was used as the standard and its content was quantified using previously established methods [27]. Pigment concentrations were compared to a 20 mg/L astaxanthin standard [28]. Calibration standards for astaxanthin were prepared to generate calibration curves for quantification. The concentrations of these pigments in the samples were determined by comparing their peak areas to those of the calibration standards. This method is based on established protocols [27,29].

2.4 Statistics and analysis

All calculations and plots were performed in an R environment (version 4.3.3). Figures were created using the ggplot2 package (version 3.5.0), while data processing was conducted using the 'tidyverse' package [30]. Smoothed model fits (method = "lm") were carried out using the geom smooth function from ggplot2 [31].

3. Results and Discussion

3.1 Phenotypic and growth changes of HTB1 under salinity stress

Microscopic observations of HTB1 cells under varying salinity conditions revealed significant morphological changes as salinity increased (Fig. 1). Under control conditions (0 ppt), the cells maintained a consistent spherical shape with dark green pigmentation and at 20 ppt, cells somewhat retained their green color. However, they appeared pale at 25, 27.5, and 30 ppt, indicating stress at higher salinities. Data from Coulter counter analysis further supported these findings, showing that cell size increased at 20 ppt but decreased at higher salinities (Fig. 2A). At 0, 17.5, and 20 ppt, cell sizes peaked at 6 μm, while cell sizes peaked at approximately 3 μm when salinity was in the range of 25-30 ppt. The presence of dual peaks at 22.5 ppt (3 and 6 μm) may represent a critical cell size transition point for HTB1 under salt stress. Elevated salinity often triggers osmotic stress, which can lead to changes in cell size, shape, and even intracellular content, as cells adapt to maintain homeostasis [15,16]. Collectively, these data imply that HTB1 may undergo morphological change and pigment loss in response to elevated salinity pressure.

The growth of HTB1 was highest at 0 ppt, declined gradually with increasing salinity, and was inhibited when the salinity exceeded 22.5 ppt (Fig. 2B). The most severe growth inhibition occurred at 30 ppt. The 20 ppt salinity appears to be the growth threshold for *Scenedesmus* species where its growth slows down [34]. It has been reported that the growth of *S. obliquus* was reduced significantly when salinity was higher than 15 ppt [35]. Taken together, elevated salinities affect the morphology, growth, and pigmentation of HTB1. HTB1 reduced cell size and pigmentation in response to osmotic stress at higher salinities and did not grow well when the salinity was higher than 22.5 ppt.

3.2 Culture color and pigment changes of HTB1 under salinity stress

The progressive change in culture color with increasing salinity was evident over the 10-day incubation period (Fig. 3). By day 2, subtle variations in color were noticeable across the salinity gradient. By day 4, the culture color shifted from green-brown to yellow-brown and ultimately to pale white as salinity levels increased from 17.5 to 30 ppt. This color pattern remained stable through days 8 and 10 (Fig. 3). Notably, one replicate at 27.5 ppt is an outlier due to an error in salinity preparation, resulting in an actual salinity of 22.5 ppt. The transition from dark green to pale white across the salinity gradient implies that HTB1 alters its pigment composition under elevated salt conditions. Interestingly, the pronounced decline in pigment abundance at 30 ppt suggests this salinity level may impair cellular functions and reduce pigment synthesis (Fig. 4). Previous studies on *S. obliquus* also documented similar color transitions from green to yellow to pale white when exposed to high salinity [34,36–38].

Salinity changes also posed a significant impact on the pigment composition of HTB1. The decreasing trends of lutein, chlorophyll *b*, beta-carotene, neoxanthin, violaxanthin, and zeaxanthin with increasing salinity (Fig. 5) suggested that elevated salinity levels adversely affected the biosynthesis or degradation of these pigments. These pigments are essential for light harvesting and photoprotection, and their reduction may reflect stress responses or impaired metabolic activities under stress, such as high light stress [39]. From 17.5 ppt to 30 ppt salinity, both lutein and chlorophyll *b* exhibited a decreasing trend in the peak area (Fig. 4). Beta-carotene decreased as salinity increased. Secondary pigments such as neoxanthin, violaxanthin, and zeaxanthin were present but generally decreased with rising salinity. Notably, canthaxanthin concentration increased from 332 ± 55 to 426 ± 57 as salinity increased from 17.5 ppt to 25 ppt, contrary to the trends of other pigments. The increased production of canthaxanthin under high light stress has been reported in *Dactylococcus dissociates* [40]. However, at 30 ppt salinity, all pigments

(including canthaxanthin) declined (Fig. 5), suggesting that pigment biosynthesis of HTB1 was inhibited. Excessive salt stress also inhibits pigment production of other microalgae like *Dunaliella salina*, *Haematococcus pluvialis* and *Scenedesmus sp*. [41].

The scatterplot between pigments and salinity shows that canthaxanthin had a positive relationship with salinity, while other pigments were negatively related to salinity (Fig. 5). The increasing trend of canthaxanthin with elevated salinity (up to 25 ppt) is particularly interesting. Ketocarotenoid is known for its antioxidant properties, canthaxanthin may play a protective role under salinity-induced oxidative stress [42]. The increase of canthaxanthin in HTB1 could be a physiological response to mitigate damage from reactive oxygen species generated under saline stress. Similar findings have been reported in other microalgae, where increased canthaxanthin production was associated with physio-chemical stress conditions [43].

3.3 Increased tolerance and biomass yield of HTB1 under 10% CO_2 incubation

Because the growth of HTB1 was inhibited with higher salinity (>22.5 ppt) (Fig. 2B), we tested the salinity range (0, 10, and 20 ppt) in the second experiment. Interestingly, HTB1 cultures with 10% CO_2 remained a dark green color at 0, 10, and 20 ppt salinity, while the cultures with ambient air changed color at 10 and 20 ppt (Fig. 6). For the cultures with ambient air, HTB1 culture changed slightly from dark green to light green at 10 ppt but changed from dark green to brownish color at 20 ppt after day 6. It was evident that HTB1 tolerated salinity stress with less change in pigment color with 10% CO_2.

Under the same salinity condition, the growth of HTB1 with 10% CO_2 outperformed that with ambient air, as shown by the OD_{750} and ash-free dry weight (AFDW) measurement (Fig. 7A and 7B). For AFDW, the mean weight of HTB1 was higher in the 10% CO_2 treatment than in the air treatment by 17.8%, 20.8%, and 20.1% for 0, 10, and 20 ppt salinity, respectively. It appears that

elevated CO_2 enhanced the salt tolerance of HTB1, particularly under 10 ppt salinity conditions. However, at salinity levels above 20 ppt, growth remained somewhat inhibited. Elevated CO_2 may help mitigate salinity stress by improving photosynthetic efficiency and pigment production [44]. It has been reported that increased CO_2 enhances stress tolerance in microalgae [45,46]. CO_2 likely plays a role in maintaining cellular functions during stress by optimizing photosynthesis and aiding in carbon fixation, which supports cellular metabolism under challenging conditions [47]. This trend was consistent across various experimental conditions, showing that CO_2 improves both biomass yield and chlorophyll concentration, even at elevated salinity levels, similar to[47]. Our results suggest that the growth of HTB1 benefits from CO_2 enrichment, especially under moderate salinity stress (at 10 ppt).

The growth difference of HTB1 under different salinities appeared to be greater by the OD measurement than the AFDW measurement (Fig. 7A vs 7B). The growth curves of HTB1 with 3 different salinities measured by OD_{750} did not always align with those measured by AFDW. This discrepancy is likely due to the difference in methodology. Optical density at 750 nm is a rapid, non-destructive method to estimate cell density based on light absorption. It provides an indirect estimation of biomass by measuring the turbidity caused by suspended cell particles. OD_{750} can be influenced by factors such as cell size, shape, and intracellular components. Changes in morphology, pigment concentration, or extracellular compounds can cause OD readings to vary, even when actual biomass remains relatively stable. In contrast, AFDW measures the organic biomass directly, excluding inorganic materials like salts or minerals. This makes AFDW a more accurate method for assessing the organic content of the cells, although it does not account for changes in cell morphology or pigment content that might affect OD measurements.

3.4 Altered pigment profiles of HTB1 under 10% CO_2 incubation

The HPLC analysis revealed various pigment profiles of HTB1 under different treatments of ambient air and elevated 10% CO_2 concentrations (Fig. 8). Eight key pigments were identified including zeaxanthin, violaxanthin, neoxanthin, lutein, canthaxanthin, chlorophyll *b*, chlorophyll *a*, and beta-carotene. Interestingly, the change of pigment composition with salinity differed between the air and 10% CO_2 groups. Under ambient air conditions, the content of major pigments such as lutein, chlorophyll *a*, and chlorophyll *b* declined as salinity increases (Fig. 9A). This trend was consistent with the results from Fig. 4 and 5, suggesting that increased salinity negatively affected pigment content. In corroboration, a decline in photosynthetic pigment biosynthesis under osmotic stress was reported in other photosynthetic microorganisms such as in cyanobacteria [48]. The pigment composition of HTB1 grown with 10% CO_2 revealed an opposite trend in contrast to those grown with air (Fig. 9B). Lutein and chlorophyll b contents increased with salinity levels, including 0 ppt (lutein: 0.14 ± 0.12 w/w, chlorophyll b: 0.07 ± 0.06 w/w), 10 ppt (lutein: 0.19 ± 0.01 w/w, chlorophyll b: 0.1 ± 0.01 w/w), and 20 ppt (lutein: 0.19 ± 0.03 w/w, chlorophyll b: 0.08 ± 0.005 w/w), suggesting that elevated CO_2 might mitigate the effects of salinity stress and boost pigment storage and photosynthetic efficiency. The increase in canthaxanthin under the CO_2 treatment may further indicate a protective role for this carotenoid, which is known to act as an antioxidant and photo-protectant [50,51].

The trends observed in canthaxanthin content (Fig. 9) also align with previous research suggesting that this carotenoid may accumulate in response to stress conditions, particularly in the presence of CO_2 [52]. The role of canthaxanthin in photoprotection could be a key factor in algal survival under stressful environments, such as high-salinity conditions.

3.5 Pigment yield

Six pigments including neoxanthin, violaxanthin, zeaxanthin, beta-carotene, canthaxanthin, and lutein exhibited distinct concentration patterns across salinity levels of 0, 10, and 20 ppt under ambient air and elevated carbon dioxide (CO_2) conditions (Fig. 10). Except for beta-carotene and lutein at 0 ppt, pigment concentrations were generally higher under 10% CO_2 compared to air. This suggests that elevated CO_2 enhanced HTB1's photosynthetic capacity by increasing pigment production, consistent with the significantly greater ash-free dry weight (AFDW) observed under 10% CO_2 relative to air (Fig. 7B).

The six pigments responded to salinity change differently under elevated CO_2. With 10% CO_2, neoxanthin and beta-carotene peaked at 10 ppt (Fig. 10), while violaxanthin and zeaxanthin were most abundant at 0 ppt. Canthaxanthin, in contrast, steadily increased with rising salinity, reaching its highest level at 20 ppt. Lutein was highest at salinities of 10 and 20 ppt under elevated CO_2. Overall, elevated CO_2 enhanced the production of most pigments, particularly at moderate salinity levels. These increases likely provide photoprotective and antioxidant benefits, enabling HTB1 to better cope with environmental stress. The distinct responses of individual pigments highlight how HTB1 refines its metabolic processes to adapt to varying salinity and CO_2 conditions.

4 Conclusion

When HTB1 was cultivated with ambient air, salinity changes significantly influenced its pigment composition. The observed decline in lutein, chlorophyll *b*, beta-carotene, neoxanthin, violaxanthin, and zeaxanthin levels with increased salinity suggests that higher salt concentrations may impair the biosynthesis and/or degradation of these pigments. As salinity increased, HTB1 cells shrank in size, and the culture color shifted progressively from green to brown, yellow-brown, and eventually to pale white or yellow.

Interestingly, canthaxanthin levels exhibited a rising trend from 17.5 ppt to 25 ppt, contrasting with the responses of other pigments under salt stress. The elevation of canthaxanthin levels under salt stress may serve as a physiological adaptation, potentially helping HTB1 in saline conditions. The growth of HTB1 declined with increasing salinity and was notably inhibited at levels above 22.5 ppt.

The growth inhibition was less severe under 10% CO_2 than ambient air, indicating that elevated CO_2 may alleviate salt stress in HTB1. Furthermore, both lutein and canthaxanthin yields increased with higher salinity when HTB1 was cultivated in 10% CO_2. This study provides valuable insights into the effects of salt stress on algal physiology and pigment production and deepens our understanding of the physiological responses of *S. obliquus* to salt stress under air and elevated CO_2 conditions.

Author declaration

Submission of an article implies that the work described has not been published previously (except in the form of an abstract or as part of a published lecture or academic thesis), that it is not under consideration for publication elsewhere, that its publication is approved by all authors and tacitly or explicitly by the responsible authorities where the work as carried out, and that, if accepted, it will not be published elsewhere in the same form, in English or in any other language, without the written consent of the copyright holder. By attaching this Declaration to the submission, the corresponding author certifies that:

- The manuscript represents original and valid work and neither this manuscript nor one with substantially similar content under the same authorship has been published or is being considered for publication elsewhere.
- Every author has agreed to allow the corresponding author to serve as the primary correspondent with the editorial office, and to review the edited typescript and proof.
- Each author has given final approval of the submitted manuscript and order of authors. Any subsequent change to authorship will be approved by all authors.
- Each author has participated sufficiently in the work to take public responsibility for all the content.

Declaration of competing interest

The authors declare that they have no known competing financial interests or personal relationships that could have appeared to influence the work reported in this paper.

References

[1] O. Pulz, W. Gross, Valuable products from biotechnology of microalgae, Appl. Microbiol. Biotechnol. 65 (2004) 635–648.

[2] N. Mallick, S. Mandal, A.K. Singh, M. Bishai, A. Dash, Green microalga *Chlorella vulgaris* as a potential feedstock for biodiesel, J. Chem. Technol. Biotechnol. 87 (2012) 137–145.

[3] M. Orosa, E. Torres, P. Fidalgo, J. Abalde, Production and analysis of secondary carotenoids in green algae, J. Appl. Phycol. 12 (2000) 553–556.

[4] Z. Cohen, A. Richmond, Products of Microalgae, Handbook of Microalgae Mass Culture, CRC Press Fla. (1986).

[5] S. Khanra, M. Mondal, G. Halder, O.N. Tiwari, K. Gayen, T.K. Bhowmick, Downstream processing of microalgae for pigments, protein and carbohydrate in industrial application: A review, Food Bioprod. Process. 110 (2018) 60–84.

[6] M.R. Gauthier, G.N.A. Senhorinho, J.A. Scott, Microalgae under environmental stress as a source of antioxidants, Algal Res. 52 (2020) 102104.

[7] K. Skjånes, C. Rebours, P. Lindblad, Potential for green microalgae to produce hydrogen, pharmaceuticals and other high value products in a combined process, Crit. Rev. Biotechnol. 33 (2013) 172–215.

[8] C. Paliwal, M. Mitra, K. Bhayani, S.V. Bharadwaj, T. Ghosh, S. Dubey, S. Mishra, Abiotic stresses as tools for metabolites in microalgae, Bioresour. Technol. 244 (2017) 1216–1226.

[9] E.-S. Salama, H.-C. Kim, R.A. Abou-Shanab, M.-K. Ji, Y.-K. Oh, S.-H. Kim, B.-H. Jeon, Biomass, lipid content, and fatty acid composition of freshwater *Chlamydomonas mexicana* and *Scenedesmus obliquus* grown under salt stress, Bioprocess Biosyst. Eng. 36 (2013) 827–833.

[10] K. Chokshi, I. Pancha, A. Ghosh, S. Mishra, Nitrogen starvation-induced cellular crosstalk of ROS-scavenging antioxidants and phytohormone enhanced the biofuel potential of green microalga *Acutodesmus dimorphus*, Biotechnol. Biofuels 10 (2017) 1–12.

[11] X. Ji, J. Cheng, D. Gong, X. Zhao, Y. Qi, Y. Su, W. Ma, The effect of NaCl stress on photosynthetic efficiency and lipid production in freshwater microalga—*Scenedesmus obliquus* XJ002, Sci. Total Environ. 633 (2018) 593–599.

[12] J. Li, D. Han, D. Wang, K. Ning, J. Jia, L. Wei, X. Jing, S. Huang, J. Chen, Y. Li, Choreography of transcriptomes and lipidomes of *Nannochloropsis* reveals the mechanisms of oil synthesis in microalgae, Plant Cell 26 (2014) 1645–1665.

[13] C.-J. Yun, K.-O. Hwang, S.-S. Han, H.-G. Ri, The effect of salinity stress on the biofuel production potential of freshwater microalgae *Chlorella vulgaris* YH703, Biomass Bioenergy 127 (2019) 105277.

[14] M.F. Assuncao, R. Amaral, C.B. Martins, J.D. Ferreira, S. da Ressurreicao, S.D. Santos, J.M. Varejao, L. Santos, Determination of antioxidant capacity across different taxa of microalgae, in: Eur. J. Phycol., Taylor & Francis LTD, 2015: pp. 156–156.

[15] A. Solovchenko, I. Khozin-Goldberg, High-CO_2 tolerance in microalgae: possible mechanisms and implications for biotechnology and bioremediation, Biotechnol. Lett. 35 (2013) 1745–1752.

[16] J. Yang, C. Zhang, H. Hu, Screening high CO_2-tolerant oleaginous microalgae from genera *Desmodesmus* and *Scenedesmus*, Appl. Biochem. Biotechnol. 192 (2020) 211–229.

[17] M. Zhang, H. Wang, F. Chen, Time-resolved transcriptome analysis of *Scenedesmus obliquus* HTB1 under 10% CO_2 condition, Microb. Biotechnol. 16 (2023) 448–462.

[18] D.J. Farrelly, C.D. Everard, C.C. Fagan, K.P. McDonnell, Carbon sequestration and the role of biological carbon mitigation: a review, Renew. Sustain. Energy Rev. 21 (2013) 712–727.

[19] V. Bhola, F. Swalaha, R. Ranjith Kumar, M. Singh, Fjij. Bux, Overview of the potential of microalgae for CO_2 sequestration, Int. J. Environ. Sci. Technol. 11 (2014) 2103–2118.

[20] A. Guldhe, B. Singh, I. Rawat, K. Permaul, F. Bux, Biocatalytic conversion of lipids from microalgae *Scenedesmus obliquus* to biodiesel using *Pseudomonas* fluorescens lipase, Fuel 147 (2015) 117–124.

[21] M. Lürling, E. Van Donk, Grazer-induced colony formation in *Scenedesmus*: are there costs to being colonial?, Oikos 88 (2000) 111–118.

[22] M.-H. Park, C.-H. Park, Y.B. Sim, S.-J. Hwang, Response of *Scenedesmus quadricauda* (Chlorophyceae) to salt stress considering nutrient enrichment and intracellular proline accumulation, Int. J. Environ. Res. Public. Health 17 (2020) 3624.

[23] W.-K. Yong, K.-S. Sim, S.-W. Poong, D. Wei, S.-M. Phang, P.-E. Lim, Physiological and metabolic responses of *Scenedesmus quadricauda* (Chlorophyceae) to nickel toxicity and warming, 3 Biotech 9 (2019) 1–11.

[24] P. Kaewkannetra, P. Enmak, T. Chiu, The effect of CO_2 and salinity on the cultivation of *Scenedesmus obliquus* for biodiesel production, Biotechnol. Bioprocess Eng. 17 (2012) 591–597.

[25] Z. Liu, F. Zhang, F. Chen, High throughput screening of CO_2-tolerating microalgae using GasPak bags, Aquat. Biosyst. 9 (2013) 1–7.

[26] X. Han, N. Rusconi, P. Ali, K. Pagkatipunan, F. Chen, Nutrients extracted from chicken manure accelerate growth of microalga *Scenedesmus obliquus* HTB1, Green Sustain. Chem. 7 (2017) 101–113.

[27] J.-P. Yuan, F. Chen, Purification of trans-astaxanthin from a high-yielding astaxanthin ester-producing strain of the microalga *Haematococcus pluvialis*, Food Chem. 68 (2000) 443–448.

[28] K. Ramarui, Improving *Haematococcus pluvialis* growth and astaxanthin production through chemical mutagenesis, University of Maryland, Baltimore County, 2019.

[29] T.T. Hanai, HPLC: a practical guide, Royal Society of Chemistry, 2007.

[30] H. Wickham, W. Chang, M.H. Wickham, Package 'ggplot2,' create elegant data vis. using Gramm. Graph. Version 2 (2016) 1–189.

[31] H. Wickham, Tidyverse: Easily install and load the 'tidyverse,' R Package Version 1 (2017) 2017.

[32] H. Chen, A. Sosa, F. Chen, Growth and cell size of microalga *Auxenochlorella protothecoides* AS-1 under different trophic modes, Microorganisms 12 (2024) 835.

[33] R.A. Craigie, T. Cavalier-Smith, Cell volume and the control of the *Chlamydomonas* cell cycle, J. Cell Sci. 54 (1982) 173–191.

[34] W. Elloumi, A. Jebali, A. Maalej, M. Chamkha, S. Sayadi, Effect of mild salinity stress on the growth, fatty acid and carotenoid compositions, and biological activities of the thermal freshwater microalgae *Scenedesmus sp*., Biomolecules 10 (2020) 1515.

[35] S. Calhoun, B. Kamel, S. Edmundson, O. Holguin, P. Mach, Z. Mckie-Krisberg, L. Baumgart, I. Blaby, B. Bowen, C. Chen, A multi-omic characterization of the physiological responses to salt stress in *Scenedesmus obliquus* UTEX393, (2023).

[36] F.A. Amiri, N.A. Amiri, P. Karimi, A. Eslami, L. Faravardeh, M. Rafiee, A. Ghasemi, Bioaugmentation of bio-slurry reactor containing pyrene contaminated soil by engineered *Pseudomonas putida* KT2440, Water. Air. Soil Pollut. 235 (2024) 355.

[37] G.N. Hotos, D. Avramidou, The effect of various salinities and light intensities on the growth performance of five locally isolated microalgae [*Amphidinium carterae*, *Nephroselmis* sp., *Tetraselmis* sp. (var. red pappas), *Asteromonas gracilis* and *Dunaliella* sp.] in laboratory batch cultures, J. Mar. Sci. Eng. 9 (2021) 1275.

[38] P. Shetty, M.M. Gitau, G. Maróti, Salinity stress responses and adaptation mechanisms in eukaryotic green microalgae, Cells 8 (2019) 1657.

[39] A. Pinnola, The rise and fall of light-harvesting complex stress-related proteins as photoprotection agents during evolution, J. Exp. Bot. 70 (2019) 5527–5535.

[40] D. Rojas-Villalta, D. Rojas-Rodríguez, M. Villanueva-Ilama, R. Guillén-Watson, F. Murillo-Vega, O. Gómez-Espinoza, K. Núñez-Montero, Exploring extremotolerant and extremophilic microalgae: New Frontiers in Sustainable Biotechnological Applications, Biology 13 (2024) 712.

[41] Y. Ren, H. Sun, J. Deng, J. Huang, F. Chen, Carotenoid production from microalgae: biosynthesis, salinity responses and novel biotechnologies, Mar. Drugs 19 (2021) 713.

[42] X.-M. Sun, L.-J. Ren, Q.-Y. Zhao, X.-J. Ji, H. Huang, Microalgae for the production of lipid and carotenoids: a review with focus on stress regulation and adaptation, Biotechnol. Biofuels 11 (2018) 1–16.

[43] A.K. Minhas, P. Hodgson, C.J. Barrow, A. Adholeya, A review on the assessment of stress conditions for simultaneous production of microalgal lipids and carotenoids, Front. Microbiol. 7 (2016) 546.

[44] J. Masojídek, K. Ranglova, G.E. Lakatos, A.M. Silva Benavides, G. Torzillo, Variables governing photosynthesis and growth in microalgae mass cultures, Processes 9 (2021) 820.

[45] E.A. Chunzhuk, A.V. Grigorenko, S.V. Kiseleva, N.I. Chernova, K.G. Ryndin, V. Kumar, M.S. Vlaskin, The influence of elevated CO2 concentrations on the growth of various microalgae strains, Plants 12 (2023) 2470.

[46] E.A. Chunzhuk, A.V. Grigorenko, S.V. Kiseleva, N.I. Chernova, M.S. Vlaskin, K.G. Ryndin, A.V. Butyrin, G.N. Ambaryan, A.O. Dudoladov, Effects of light intensity on the growth and biochemical composition in various microalgae grown at high CO_2 concentrations, Plants 12 (2023) 3876.

[47] T. de Marchin, M. Erpicum, F. Franck, Photosynthesis of *Scenedesmus obliquus* in outdoor open thin-layer cascade system in high and low CO_2 in Belgium, J. Biotechnol. 215 (2015) 2–12.

[48] P.H. Moisander, E. McClinton Iii, H.W. Paerl, Salinity effects on growth, photosynthetic parameters, and nitrogenase activity in estuarine planktonic cyanobacteria, Microb. Ecol. (2002) 432–442.

[49] M. Giordano, J. Beardall, J.A. Raven, CO_2 concentrating mechanisms in algae: mechanisms, environmental modulation, and evolution, Annu Rev Plant Biol 56 (2005) 99–131.

[50] R.T. Lorenz, G.R. Cysewski, Commercial potential for *Haematococcus* microalgae as a natural source of astaxanthin, Trends Biotechnol. 18 (2000) 160–167.

[51] A. Richmond, Handbook of Microalgal Culture: Biotechnology and Applied Phycology, Wiley Online Library, 2004.

[52] R. Mahadi, S. Kim, D.P.A. Ilhamsyah, L.P.S. Vahisan, A.L. Narasimhan, G.W. Park, S.Y. Lee, Y.-K. Oh, Rapid accumulation of astaxanthin in *Haematococcus pluvialis* induced by mild hydrostatic pressure, Biotechnol. Bioprocess Eng. 28 (2023) 345–351.